CHAPTER -7

LCF Behaviour of Thermal Barrier Coated Inconel 617 Alloy

7.1 Introduction

This chapter presents the effect of thermal barrier coating (TBC) on low cycle fatigue behaviour of Inconel 617 alloy at 850^{o}C at different strain amplitudes in the regime of ±0.2% to ±0.5%. Yttria Stabilised Zirconia (YSZ) thermal barrier coatings possess higher melting point and lower thermal conductivity than those of the substrate nickel base super alloys and protect the base material from high temperature exposure. A bond coat is applied before applying TBC to compensate the difference of thermal stresses between the substrate and TBC, and to provide adherence with the TBC. These thermal barrier coatings reduce the exposure temperature of the base metal by 100 to 200^{o}C based on the thickness of the coating layer, the more is the thickness, higher is the reduction in temperature. This helps in increasing durability of the material at the same service temperature with longer life or increase the service temperature of the alloy if the creep strength is sufficient. These TBC coatings can also provide good oxidation and corrosion resistance. The ceramic powder particles are melted in the plasma arc and are sprayed on to the substrate, where the particles adhere to the surface of the substrate mechanically. This process generates voids or porosity in the layer which may appear as micro cracks and decrease the thermal conductivity of the coating when compared to that of the solid coating of YSZ.

The coating acts as an insulation layer and also helps in accommodating thermal and mechanical strains. As the values of modulus of elasticity and thermal expansion coefficient are generally different for both the substrate and TBC, there is always a possibility of spalling or delamination of the coating under cyclic loading at high temperatures which affects the performance of the coating. In the present chapter, the effect of TBC coating on LCF behaviour of Inconel 617 alloy is presented. Detailed fracture and deformation behaviour under cyclic loading is also discussed in comparison

with those of the LCF tested samples without coating.

7.2 Methodology

Thermal barrier coating of Yttria (8%) stabilised Zirconia (YSZ) was deposited on the fatigue samples machined from the solution annealed material using atmospheric plasma spray (APS) coating process. Fatigue samples were initially grit blasted using alumina powder (Al_2O_3) and then deposited with a bond coat of NiCrAlY (Ni-22Cr-10Al-1Y, wt.%) to a thickness of around 40 μm. The top coat (TBC) was formed on the bond coat using powdered Zirconia (ZrO_2) containing 8 wt. % of Yttria (Y_2O_3) up to a thickness of 80 μm. Minimum thickness was coated on the sample as mounting of the extensometer during LCF testing on the sample is practically difficult with increasing thickness. Effect of strain amplitude on the fatigue life of the TBC coated samples was studied by conducting LCF testing at strain amplitudes ranging from ±0.20% to ±0.50% at 850^{o}C.

7.3 Initial Characterization

The gauge section of the TBC coated fatigue samples was sectioned transversely and observed under SEM to reveal the coating thickness of bond coat as well as the top coat. Fig. 7.1a shows the SEM micrograph of the cross section indicating the average thickness of NiCrAlY bond coat as ≈40μm and that of the TBC top coat as ≈80μm. Both the coatings layers were observed to possess some porosity as the coating was done by the atmospheric plasma spray (APS) process. Fig. 7.1b shows the morphology and topography of the TBC ceramic coating in magnified view which indicates the existence of porosity, which is desirable to some extent for compensating thermal strains. SEM-EDS analysis of the TBC is shown in Fig. 7.1c which confirms the composition of the layer consisting of 7.3% (by wt.) Yttria and 92.7% (by wt.) Zirconia.

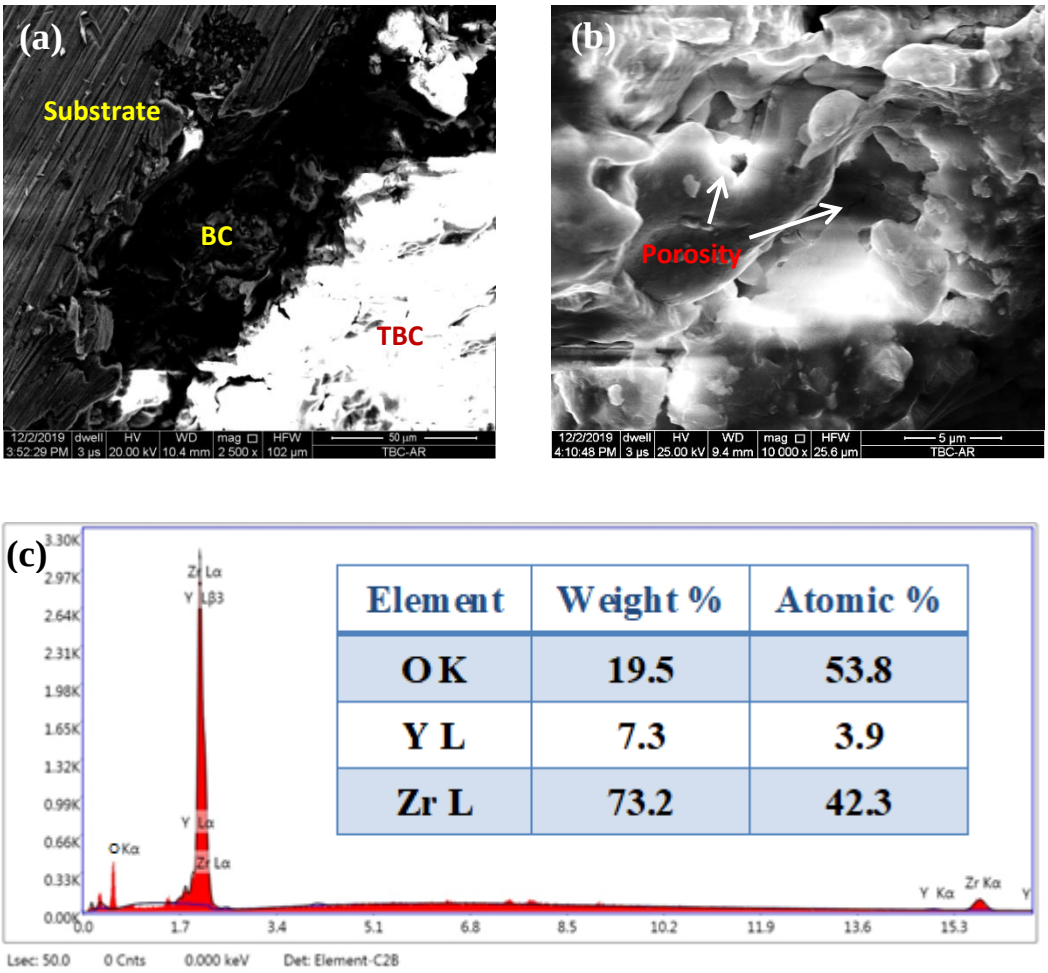

Fig. 7.1: SEM micrographs showing (a) the transverse section of the Inconel 617 alloy fatigue sample coated with bond coat (BC) and thermal barrier coating (TBC) (b) morphology of TBC coating indicating porosity and (c) SEM-EDS analysis of the TBC.

7.4 Cyclic Stress Response

The variation of tensile stress amplitude with respect to number of cycles (*N*) for the samples without and with TBC during cyclic loading at strain amplitudes ranging from ±0.20% to ±0.50% at 850^{o}C are presented in Figs. 7.2a and 7.2b respectively. Continuous cyclic hardening is observed in both the conditions for all the strain amplitudes. No significant variation in the rate of hardening with respect to strain amplitude was observed in the samples coated with TBC. It can be seen from the curves that the stress amplitude increased with increase in the strain amplitude for both the

conditions of the samples which is the same as the normal behaviour observed in most of the alloys. Table 7.1 presents the LCF data of the both samples without and with TBC, tested at various strain amplitudes at 850^{o}C. Increase in the fatigue life (N_f) at low strain amplitude (±0.20%) was observed in TBC coated samples. Slight improvement in life was observed at the intermediate strain amplitudes. There was no improvement in life for TBC coated samples at high strain amplitude ((±0.50%). The ratio of N_i/N_f for all the conditions is above 0.82, hence the half life cycle hysteresis loop data is not influenced by the crack propagation stage. It can be observed from the data of half-life cycle, presented in Table 7.1, the plastic strain amplitude found to be increased in the samples with coating at respective strain amplitude in comparison with the values found in samples without coating. Stress amplitude also followed the same trend. The values of degree of hardening (ΔH) were found to be higher for the coated samples in comparison with the values for the uncoated samples at all strain amplitudes studied.

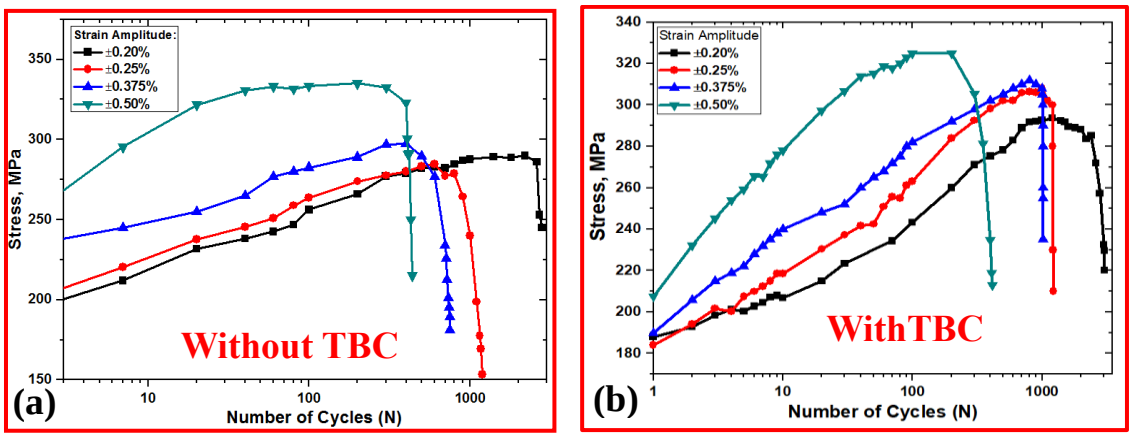

Fig. 7.2: Cyclic stress response curves of the Inconel 617 alloy fatigue samples tested at 850^{o}C and at strain amplitudes ranging from ±0.20% to ±0.50%: (a) without TBC and (b) with TBC.

Table 7.1: LCF data of the Inconel 617 Alloy Without and With TBC Tested at 850°C.

$\Delta\varepsilon_t/2$	N_i (Cycles)	N_f (Cycles)	N_i/N_f	$\Delta\varepsilon_p/2$	$\Delta\sigma/2$ (MPa)	σ_{max}	ΔH
850°C – Without TBC							
0.0020	2350	2600	0.90	0.00035	260	283	0.29
0.0025	1023	1190	0.85	0.00095	272	289	0.48
0.00375	820	973	0.84	0.00175	295	300	0.45
0.0050	390	435	0.89	0.00290	350	340	0.39
850°C – With TBC							
0.0020	2835	3043	0.93	0.00045	297	293	0.67
0.0025	1020	1235	0.82	0.00098	315	303	0.65
0.00375	860	1022	0.84	0.00190	323	311	0.68
0.0050	375	425	0.88	0.00302	345	331	0.71

Fig. 7.3 shows the cyclic stress-strain data, the plot between the stress amplitude ($\Delta\sigma/2$) and the plastic strain amplitude ($\varepsilon_p/2$), obtained from the vertices of the hysteresis loops for the TBC coated samples along with superimposed cyclic stress strain data points for the samples without TBC. Half-life cycle hysteresis loops of respective strain amplitude are considered to determine the data points for cyclic stress-strain behaviour. It clearly indicates that the TBC samples curve is at higher stress level than the curve without coated samples, which indicates more hardening samples with TBC. Equation (5.2) was used to determine the cyclic stress-strain parameters. The best fit linear regression method gives cyclic strength coefficient (K') and cyclic strain hardening exponent (n') as given in Table 7.2. It can be seen that the n' value is higher for samples tested with TBC coating, whereas K' value is less in comparison with samples tested without TBC.

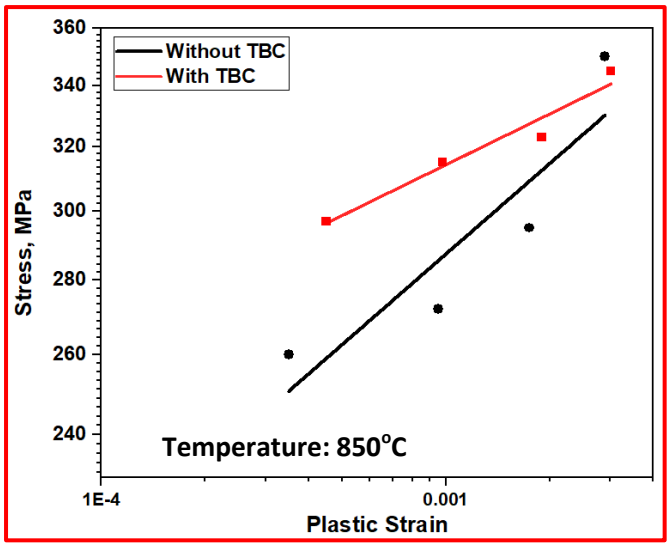

Fig. 7.3: Stress -plastic strain plots for Inconel 617 alloy without TBC and with TBC.

7.5 Strain-Life Behaviour

Fig. 7.4 shows the log-log plot of the plastic strain amplitude ($\Delta\varepsilon_p/2$) and number of reversals to failure ($2N_f$) for the samples tested without and with TBC. Linear behaviour can be observed for the both conditions. It can be inferred that it follows Coffin-Manson relationship as given by the equation

$$\Delta\varepsilon_p/2 = \varepsilon'_f (2N_f)^c \quad \text{----------} \quad (7.1)$$

where ε'_f and c are fatigue ductility coefficient and fatigue ductility exponent respectively. The parameters were evaluated using regression analysis (least square fitting) and they are listed in Table 7.2.

Table 7.2: Cyclic Stress-Strain Parameters and Coffin-Manson Parameters.

Condition	K'	n'	ε'_f	c
Without TBC	706	0.073	1.066	-1.203
With TBC	519	0.130	0.425	-0.991

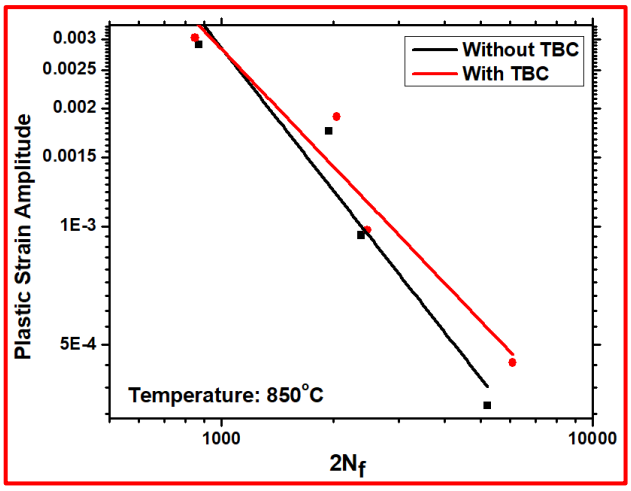

Fig. 7.4: Coffin-Manson plots for the Inconel 617 alloy without and with TBC.

7.6 Surface Morphology

Figs. 7.5a and b shows the digital photographs of the TBC samples after fatigue testing at low (±0.20%) and high strain amplitudes (±0.50%) respectively. The surface morphology of the sample at low strain amplitude clearly indicates that the coating was not spalled or delaminated, from the surface throughout the gauge section i.e. the coating was intact with the surface of the sample and no cracks were observed on the surface of the coating (Fig. 7.5a). On the other hand, the sample tested at high strain amplitude exhibited delamination or spalling of the coating from the surface and thus exposing the alloy to high temperature. Multiple cracks were observed in the coating (as shown by arrows) due to large plastic strains and/or thermal strains generated.

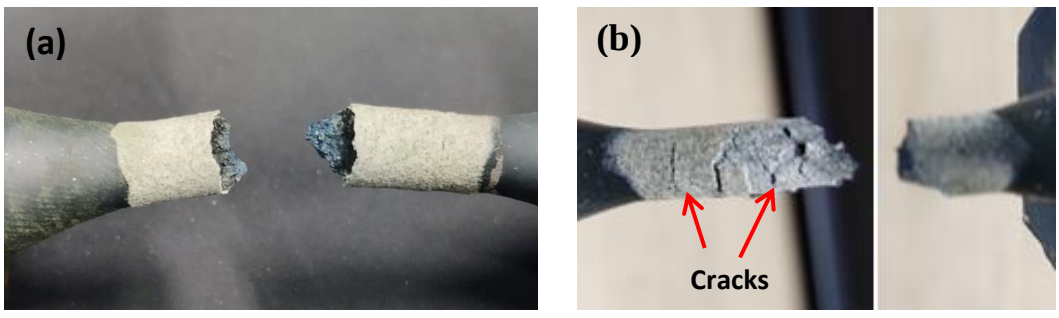

Fig. 7.5: Digital photographs of the TBC fatigue samples of Inconel 617 alloy tested at 850°C and at different strain amplitudes: (a) $\varepsilon_t/2 = \pm 0.20\%$ and (b) $\varepsilon_t/2 = \pm 0.50\%$.

SEM micrographs of longitudinal cross section of the TBC coated fatigue tested samples are shown in Fig. 7.6, which reveals adherence of coating at low strain amplitude (±0.20%) and absence of large cracks. At high strain amplitude, cross section of the samples revealed more number of voids and cracks in the coating which might have caused the exposure of the base material to the high temperature environment during testing.

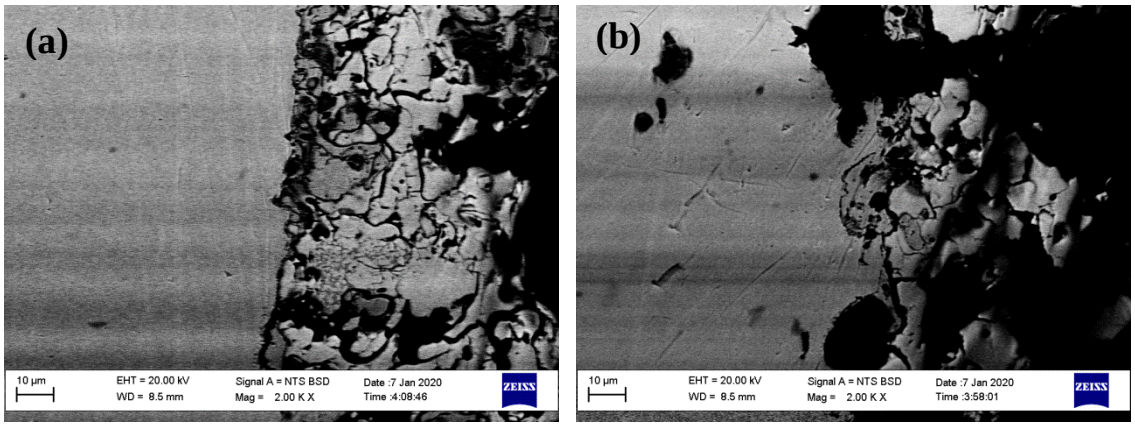

Fig. 7.6: SEM micrographs of longitudinal section of the TBC coated fatigue samples of Inconel 617 alloy tested at 850^{o}C and at different strain amplitudes: (a) $\varepsilon_t/2$ = ±0.20% and (b) $\varepsilon_t/2$ = ±0.50% revealing adherence of the coating to the surface at low strain amplitude and formation of voids in the coating at high strain amplitude.

7.7 Deformation Behaviour

Fig. 7.7 shows the TEM micrographs of the TBC samples fatigue tested at ±0.20%, revealing precipitates throughout the matrix (Fig. 7.7a) but very less in number and smaller in size (around 25 nm) compared to the precipitates observed in the samples without TBC tested at same temperature and respective strain amplitude (Fig. 5.19). The precipitates observed were indexed as $M_{23}C_6$ carbides as shown in the SAED pattern in Fig. 7.7b. As can be seen from the micrographs, these smaller sized carbides are uniformly distributed throughout the matrix. High dislocation density but inhomogeneous distribution of dislocations (forest of dislocations) can be observed as

shown by arrows. Interaction of precipitates and dislocations can also be seen in Fig. 7.7c. Magnified view of the dislocation tangles can be observed as shown in Fig. 7.7d.

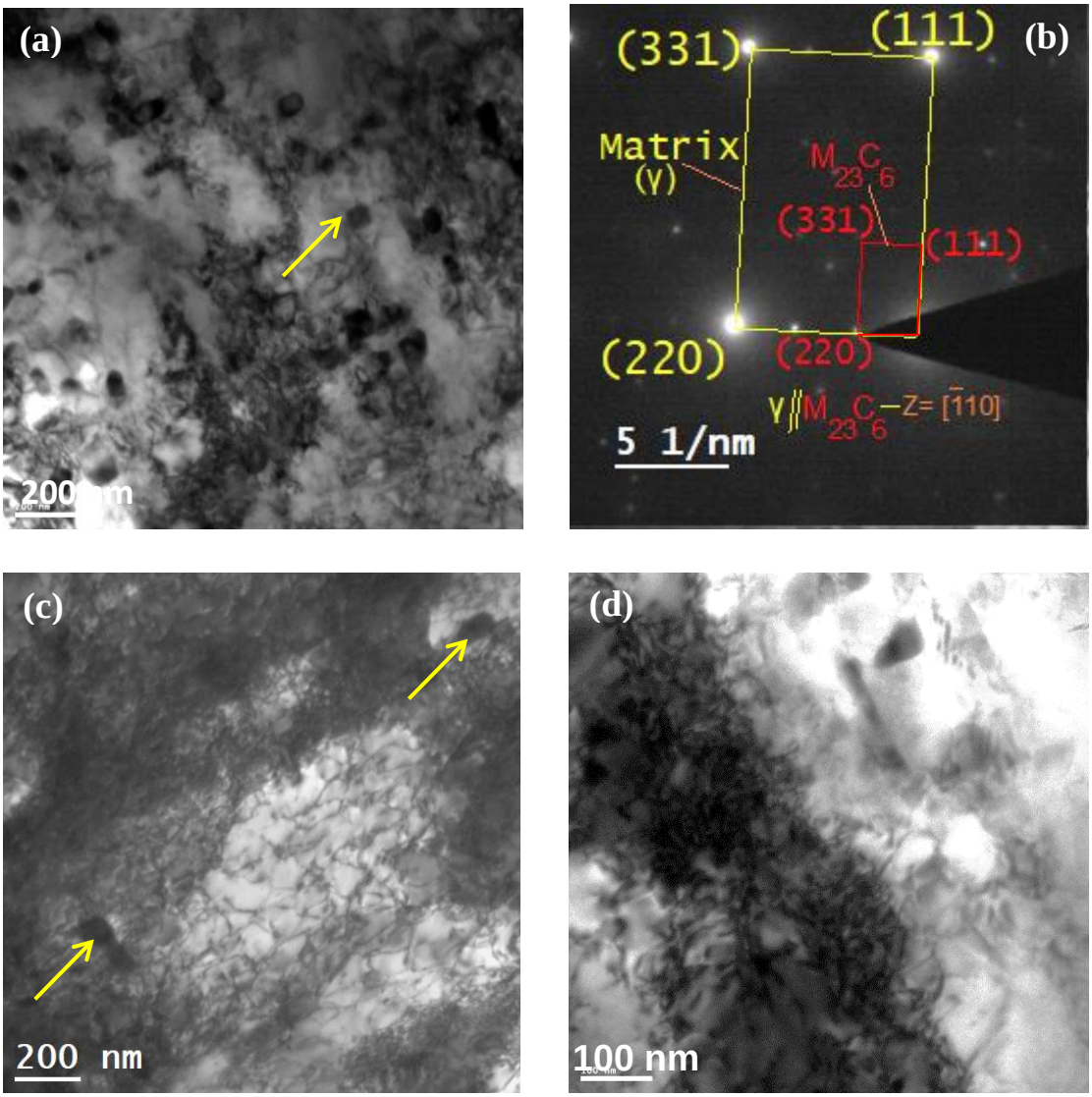

Fig. 7.7: TEM micrographs of the TBC fatigue samples of Inconel 617 alloy tested at 850^{o}C and at strain amplitude of $\varepsilon_t/2$ = ±0.20%, showing (a) the precipitates formed during testing (b) SAED pattern from $M_{23}C_6$ carbide and γ matrix (c) dislocation tangles and dislocation precipitate interaction (arrows) and (d) magnified view of the dislocation tangles shown in (c).

Fig. 7.8 shows the TEM micrographs of the TBC samples fatigue tested at higher strain amplitude (±0.50%), which indicate the presence of precipitates but much lesser in number and smaller in size than those observed in the sample tested at low strain amplitude (Figs. 7.8a and b). The dislocation density is also found to be less in

comparison to that observed in samples tested at low strain amplitude. The dislocation tangles are also uniformly distributed. Precipitate dislocation interaction can be seen in Figs. 7.8c and d.

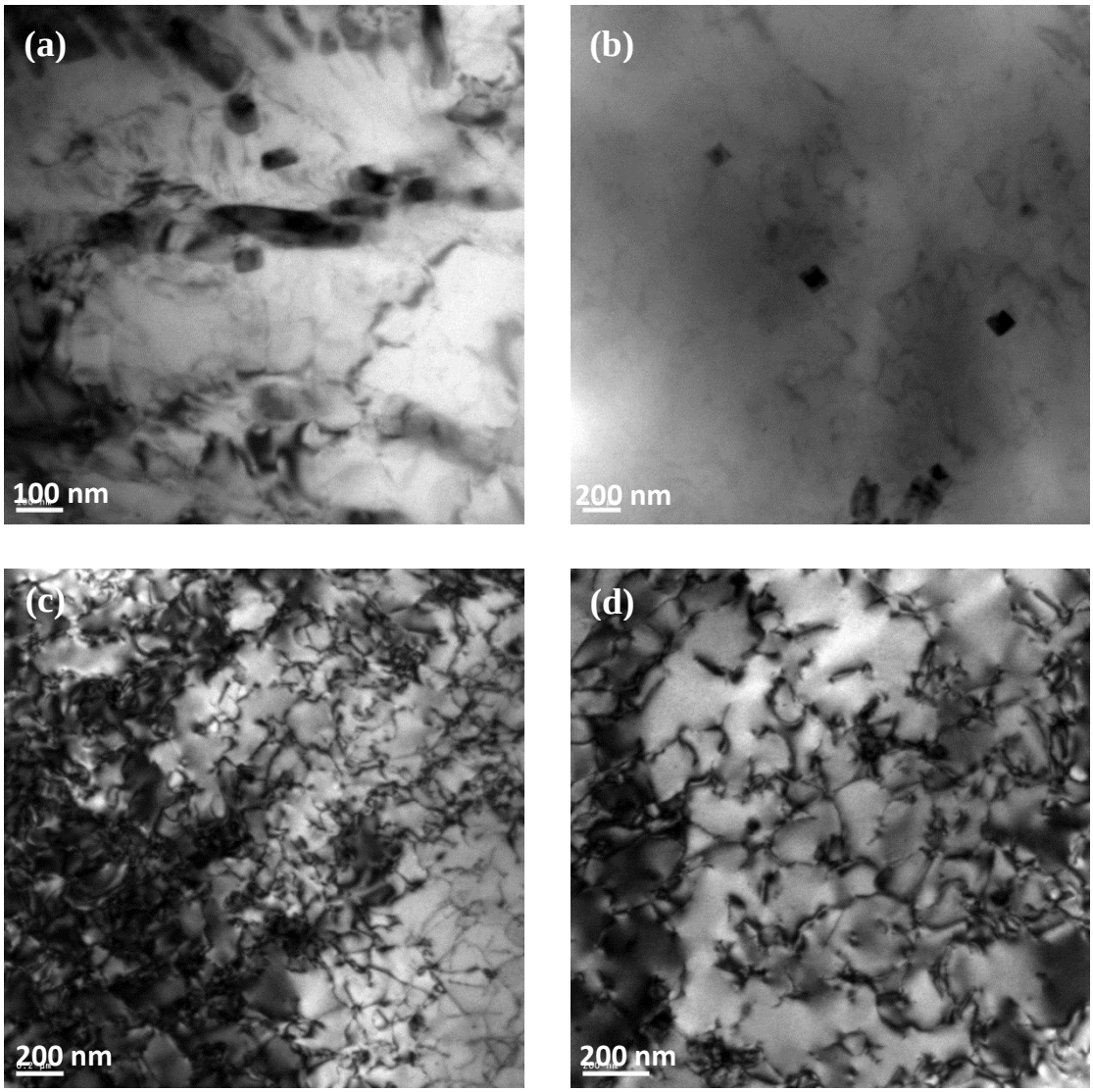

Fig. 7.8: TEM micrographs of the TBC fatigue samples of Inconel 617 alloy tested at 850^{o}C and at strain amplitude of $\varepsilon_t/2 = \pm 0.50\%$, showing: (a) the precipitates formed during testing (b) lesser number and finer size of precipitates than those at lower strain amplitude (c) dislocation tangles and dislocation precipitate interaction and (d) magnified view of the dislocation tangles shown in (c).

7.8 Fracture Behaviour

Figs. 7.9a-d show the SEM fractographs of the TBC samples tested at strain amplitude of $\varepsilon_t/2 = \pm 0.20\%$. Multiple crack initiation sites can be observed in Fig. 7.9a. The magnified view of the edge of the sample as given in Fig. 7.9b reveals the adherence of the bond coat and TBC with the substrate metal and no crack propagation from the TBC into the substrate. No delamination of the bond between bond coat and TBC can also be seen. Fig. 7.9c clearly shows the crack initiation sites from the region between the bond coat and the substrate. Fig. 7.9d shows one of the crack initiation sites in magnified view. The inter-striation marks can also be seen in this image as shown by arrow.

Fig. 7.10 shows the SEM fractographs of the TBC coated samples tested at strain amplitude of $\varepsilon_t/2 = \pm 0.50\%$, revealing multiple crack initiation sites as shown by arrows (Fig.7.10a). Fig. 7.10b shows magnified view of the edge portion of one of the crack initiation sites clearly indicating the cracks in TBC layer and the direction of one of the crack propagation is shown. The cracks propagated into the substrate perpendicular to the loading axis of the sample.

Fig 7.10c shows magnified view of the same location which reveals the crack propagation in detail in various coated layers. A gap can be seen in between the bond coat and the substrate. Cracks can be observed in the TBC layer propagating into the bond coat and further into the substrate. Striation can be seen as shown in the Fig. 7.10d, and interstriation spacing is found to vary from 2-4μm, similar to that observed in the samples without TBC for the same strain amplitude. But there is an increase in interstriation spacing with increase in strain amplitude.

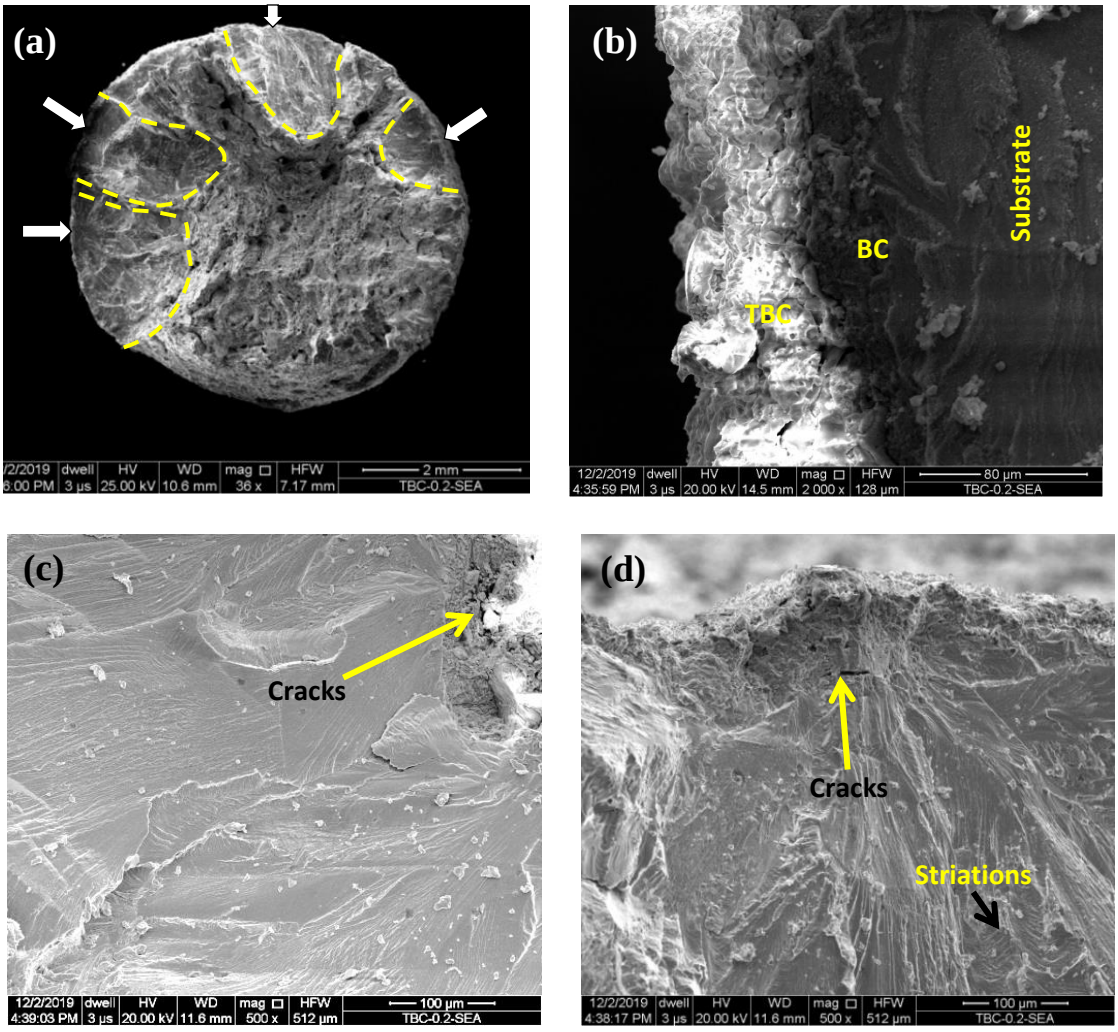

Fig. 7.9: SEM fractographs of the TBC coated fatigue samples tested at 850^{o}C and at strain amplitude of $\varepsilon_t/2$ = ±0.20%, showing (a) multiple crack initiation sites (arrows) (b) Adherence of the bond coat (BC) and TBC layer (c) crack initiation site from the region between substrate and the bond coat and absence of cracks in the TBC layer and (d) magnified view of the fracture location shown in (c) and the presence of striations and ridges (dark arrow).

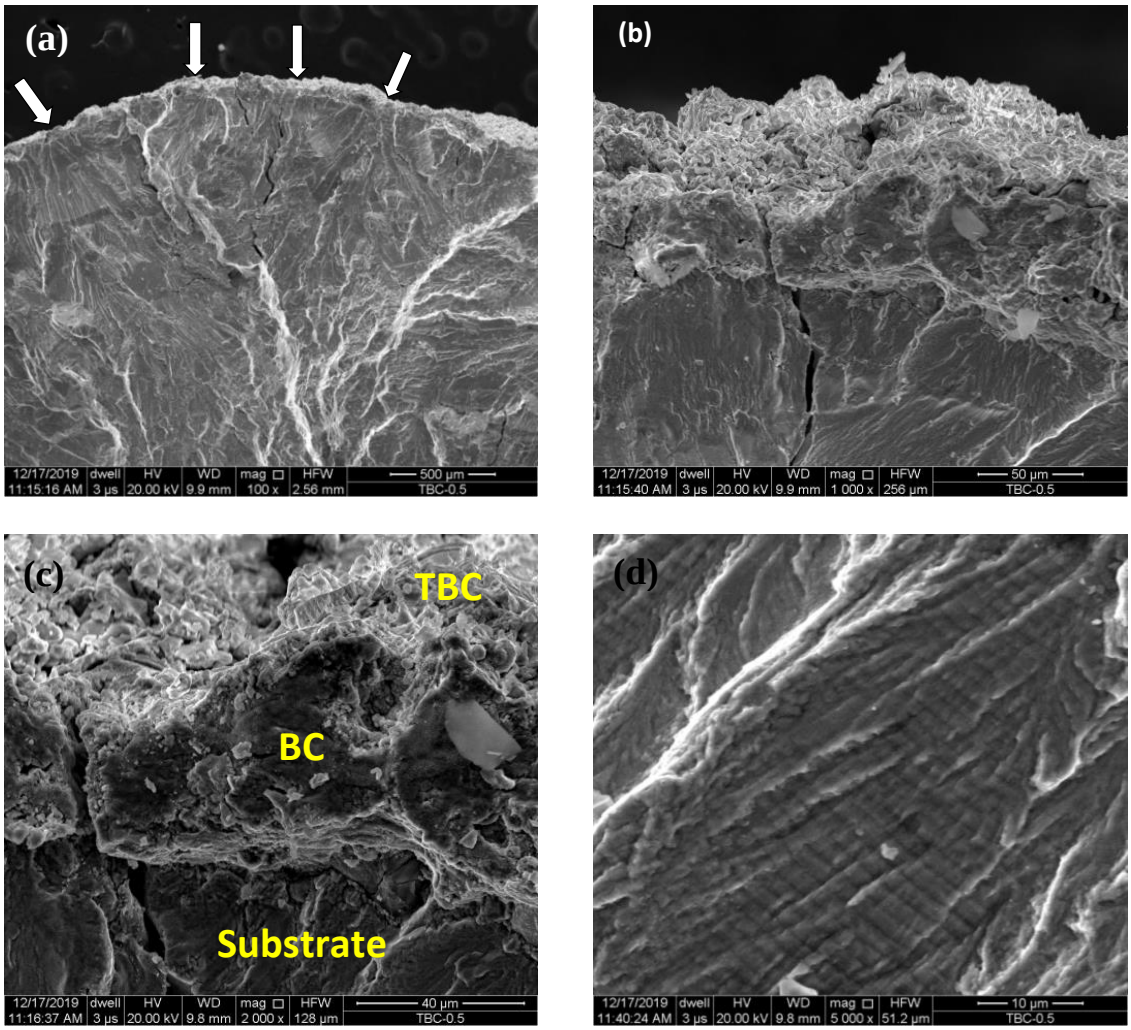

Fig. 7.10: SEM fractographs of the TBC coated fatigue samples tested at 850^{o}C and at strain amplitude of $\varepsilon_t/2$ = ±0.50%, showing: (a) multiple crack initiation sites (b) crack propagation in the TBC layer (c) crack initiation from the surface of the TBC layer and propagation into bond coat and further into substrate (d) magnified view of the fracture surface revealing striation marks and ridges.

7.9 Discussion

7.9.1 Low Cycle Fatigue Behaviour

Thermal barrier coatings improve the durability of the materials used in the high temperature applications by providing insulation to the base metal by covering the surface and reducing the temperature of the surface by 100-200^{o}C [22, 150]. These coatings also provide oxidation and corrosion resistance to the alloy. Inconel 617 alloy

is known to have good oxidation resistance for long durations. The present investigation aims at carrying out LCF studies of Inconel 617 alloy coated with TBC coating without exposing the coated material to any prior thermal exposure. In the present investigation, study of low cycle fatigue behaviour was devoted to examine the effect of strain amplitude on fatigue life of the alloy with and without TBC. Samples tested at high strain amplitude might have experienced high plastic strains in the substrate as well as in TBC. These strains caused delamination and spalling of the TBC due to low plasticity of the TBC compared to that of the substrate as TBCs are considered brittle in nature which is in good agreement with the earlier work reported on other nickel base superalloys [151-153].

The delamination of the coating that occurred during testing exposed the substrate alloy to the same temperature as that of the samples without coating. Hence there was no improvement in fatigue life observed at high strain amplitudes. The adherent coating at the low strain amplitudes protected the surface from the high temperature exposure and there was an improvement in the fatigue life by 15%. Increase in coating thickness would have further improved the fatigue life at low strain amplitudes. But due to problems associated with the mounting of the extensometer such as slot making in the coating to fix the ribs etc., a certain minimum thickness of the coating was selected for the present investigation.

The increase in the cross sectional area (considered bare sample cross sectional area) due to coating and the huge accumulation of dislocations contributed for increase in the stress amplitude for the samples with TBC, tested at the same strain amplitude as compared to the values for the samples without TBC. The degree of hardening was also more (Table 7.1), as the peak stress was more at the half-life cycle in the case of TBC coated samples in comparison to samples without coating. The presence of compressive

residual stresses generated during plasma spray coating might have also contributed for increase in the degree of hardening [154]. Though precipitation is less in the case of TBC samples, the high dislocation densities contributed for this higher degree of hardening. Coffin-Manson relationship was found to be valid in both cases. The plastic strain amplitude – number of reversals to failure ($2N_f$) plot for the LCF tested TBC samples (Fig. 7.4) illustrates the fatigue life of TBC samples was higher than the values for samples without TBC at all strain amplitudes studied except at highest strain amplitude, i.e. at $\varepsilon_{t/2}$ = ±0.50% possibly due to delamination of the coating. Similar trend has been observed in other Nickel based superalloy 713LC studied by Sulak et al. [150]. Ray et al. [151] observed high endurance limits for the superalloy Superni C263 under low stress loading (high cycle fatigue) for the TBC coated samples, whereas reduced fatigue life at high stress, and the results of the present investigation are in agreement with this observation. The premature failure was attributed to high stress crack initiation or growth in the TBC/BC layers.

7.9.2 Deformation Behaviour

The precipitation of carbides was less in the case of TBC samples compared to the samples without TBC. The precipitates were fine and uniformly distributed similar to the observations in the samples tested at 750^{o}C as reported earlier in Chapter 5, though the testing temperature is 850^{o}C in the case of TBC samples. The precipitation behaviour of TBC samples exhibited similar characteristics as that observed for the samples tested at 750^{o}C without TBC, except the number of precipitates are much less, clearly indicating the reduction in temperature of the substrate due to TBC by 100-150^{o}C. With increase in the strain amplitude, the number of precipitates decreased further due to less time available for the precipitates to form as the testing time is less.

This is in agreement with the results discussed in Section 5.10. High dislocation density in the samples tested with TBC indicates accumulation of dislocations continuously and their annihilation may not be effective (Figs. 5.19 and 5.20) and sub grain formation was also not observed. Though the recrystallization temperature was near to 800^{o}C for this alloy [53, 54], the sub grain formation did not occur due to the actual temperatures that may exist in the substrate are between 700-750^{o}C.

The presence of dislocation pileups indicates that the dynamic recovery also is not significant in the samples tested with TBC. It can be inferred that the TBC has protected the base material from any changes as both recovery as well as recrystallization temperatures were not attained during testing at 850^{o}C. The interaction of precipitates with dislocations and huge accumulation of dislocations are the main contribution factors for the cyclic hardening and increase in stress amplitude for these samples. At low strain amplitudes, higher loads are required to annihilate the dislocations under cyclic loading. This may be the reason for the observation of high dislocation density at these strain amplitudes. At high strain amplitude, the dislocations accumulation was found to be very low.

7.9.3 Fracture Behaviour

The integrity of the TBC is affected due to crack initiation at multiple sites at high strain amplitude during cyclic loading. The number of the multiple crack initiation sites increased in the tested samples with TBC compared to that in tested samples without TBC. Though more number of cracks was observed in the coating for the samples tested at high strain amplitude, very few cracks were able to propagate through the substrate. Propagation of one of the cracks is shown in Fig. 7.10c, which changed its direction during propagation into substrate. At low strain amplitudes, the crack initiation

occurred from the intermediate region of bond coat and substrate and between TBC and bond coat in some regions. Formation of thermally grown oxide (TGO) of Al_2O_3 causes weak interfaces between the bond coat and TBC and enhances the chances of crack initiation rate. The breaking of interface may cause early failure of the samples [152]. Interstriation spacing increased with increase in strain amplitude due to the high plastic strains generated at high strain amplitude. The longitudinal cross section of the TBC sample at high strain amplitude (Fig. 7.6) showed larger voids due to expansion of the coating which affected the bonding between the coating powder particles and exposed the material to high temperatures. This is the main damaging mechanism in the samples with TBC.

7.10 Chapter Summary

The summary of the present chapter is given below.

1. At low strain amplitude, LCF life of the Inconel 617 alloy with TBC was increased whereas at high strain amplitude, there was no improvement in fatigue life compared to those of samples without TBC at respective strain amplitudes.
2. The stress amplitude increased for TBC samples at all strain amplitudes in comparison to the values in the samples without TBC. Degree of hardening also increased for the TBC samples.
3. Precipitation of carbides occurred in the TBC samples though they are fine and less in number in comparison to the observations in samples without TBC. Dislocation density was increased in the TBC samples at all the strain amplitudes.
4. Cracks were initiated from the substrate alloy in the sample tested at the low

strain amplitude and the coating was found to be adherent with the base metal.

5. At high strain amplitude, delamination of the TBC coating, initiation and propagation of cracks in TBC led to early fracture. Hence, slight reduction in fatigue life was observed.
6. Inter-striation spacing was increased with increase in strain amplitude in LCF tested TBC samples.